Journal of Zhejiang University-SCIENCE A (Applied Physics & Engineering) 2025 26(7):635-651
www.jzus.zju.edu.cn; www.springer.com/journal/11582
E-mail: jzus_a@zju.edu.cn

Research Article

https://doi.org/10.1631/jzus.A2400287

Check for updates

Accuracy allocation method for five-axis machine tools based on geometric error cost sensitivity prioritizing tool direction deviation

Xiaojian LIU[1,2,3,4], Ao JIAO[3,4], Yang WANG[1,3,4]✉, Guodong YI[2,3,4]✉, Xiangyu GAO[3], Xiaochen ZHANG[5], Yiming ZHANG[2,3], Yangjian JI[2,3], Shuyou ZHANG[1,2,3,4], Jianrong TAN[1,2,3,4]

[1]*Ningbo Global Innovation Center, Zhejiang University, Ningbo 315100, China*
[2]*State Key Laboratory of Fluid Power and Mechatronic Systems, Zhejiang University, Hangzhou 310058, China*
[3]*School of Mechanical Engineering, Zhejiang University, Hangzhou 310058, China*
[4]*Zhejiang Advanced CNC Machine Tool Technology Innovation Center, Taizhou 317500, China*
[5]*Department of Mechanical Engineering, University College London, London, UK*

Abstract: Accuracy allocation is crucial in the accuracy design of machining tools. Current accuracy allocation methods primarily focus on positional deviation, with little consideration for tool direction deviation. To address this issue, we propose a geometric error cost sensitivity-based accuracy allocation method for five-axis machine tools. A geometric error model consisting of 41 error components is constructed based on homogeneous transformation matrices. Volumetric points with positional and tool direction deviations are randomly sampled to evaluate the accuracy of the machine tool. The sensitivity of each error component at these sampling points is analyzed using the Sobol method. To balance the needs of geometric precision and manufacturing cost, a geometric error cost sensitivity function is developed to estimate the required cost. By allocating error components affecting tool direction deviation first and the remaining components second, this allocation scheme ensures that both deviations meet the requirements. We also perform numerical simulation of a BC-type (*B*-axis and *C*-axis type) five-axis machine tool to validate the method. The results show that the new allocation scheme reduces the total geometric error cost by 27.8% compared to a uniform allocation scheme, and yields the same positional and tool direction machining accuracies.

Key words: Five-axis machine tool; Accuracy allocation; Geometric error modeling; Error cost sensitivity; Tool direction deviation priority

1 Introduction

Five-axis machine tools have unique advantages in complex surface machining and manufacturing, being widely used in the aerospace, aviation, automotive, and defense industries. The machining accuracy of five-axis machine tools directly reflects a country's advanced manufacturing technology level. Numerous factors affect the machining accuracy of five-axis machine tools, including geometric errors (Jiang and Cripps, 2015; Fan et al., 2024; Zhang HN et al., 2024), thermal errors (Zhu et al., 2023; Wei et al., 2024; Niu et al., 2025), and errors induced by cutting forces, servo errors, and tool wear (Yu et al., 2021; Díaz-Saldaña et al., 2023). Among these factors, geometric errors and thermal errors together account for approximately 50%–70% of the total, with geometric errors alone accounting for approximately 40% (Li et al., 2018). Geometric errors exhibit systematic characteristics, repeatability, and stability (Xia et al., 2019). Designing tolerances for geometric errors at the initial stage of machine tool development is a valid strategy for improving the machining accuracy. However, there are as many as 41 geometric error components in five-axis machine tools (Xing et al., 2019). These error components have different degrees of influence on machine tool accuracy, and require different costs to implement tolerance controls. Therefore, it is important to quantify the importance of each error component, and

✉ Yang WANG, onward@zju.edu.cn
Guodong YI, ygd@zju.edu.cn
Xiaojian LIU, https://orcid.org/0000-0001-8147-9954
Yang WANG, https://orcid.org/0000-0002-3576-1817
Guodong YI, https://orcid.org/0000-0002-7711-7982

Received June 2, 2024; Revision accepted Aug. 27, 2024;
Crosschecked June 22, 2025

design tolerances based on their importance and relative implementation costs.

To study the importance of error components on machine tool accuracy, we perform a sensitivity analysis. Sensitivity analysis involves investigating the degree to which different inputs to a model influence the uncertainty in the output (Saltelli et al., 2019) and is typically divided into two types: local and global sensitivity analyses (Zhang Z et al., 2024). Local sensitivity analysis involves examining the influence of a single parameter in the inputs on the output results. Global sensitivity analysis involves studying the variations and interactions of multiple parameters, and how these affect the output results (Liu et al., 2019); this is an effective tool for machine tool precision research. Since machine tool geometric error models typically take the geometric error values of each axis as inputs and tool positioning deviations (either positional or tool directional) as outputs, performing global sensitivity analysis is an effective way to quantify the importance of each geometric error component, identify critical error components, and guide machine tool precision design.

In recent years, scholars have conducted extensive research on machine tool accuracy using sensitivity analysis methods. For example, Song et al. (2024) proposed an error allocation method based on sensitivity analysis and an optimized genetic algorithm, which was used to allocate accuracy for a five-axis ultra-precision machine tool. Ding et al. (2023) proposed a method for analyzing geometric error influence on key gear evaluation deviations, and crucial geometric errors were identified based on the Morris sensitivity analysis method. Additionally, Niu et al. (2021) introduced an improved second-order partial correlation coefficient based on the Pearson product-moment correlation coefficient. They considered the dynamic influence of the rapid fluctuations in error parameters during the motion component's stroke on the machining accuracy. Their research provided guidance for improving the accuracy of computer numerical control (CNC) machine tool machining through a comprehensive study of the local effects, correlations, and fluctuations of geometric errors. In another study, Fan et al. (2020) divided a workpiece into five regions based on the open and twist angles, and proposed a quantitative interval sensitivity analysis method. They identified critical geometric errors in each region. Zhong et al. (2019) calculated the sensitivity of assembly errors to machine tool motion accuracy, using the partial differential method. They identified the most critical assembly errors and improved machine tool motion accuracy by adjusting the tightness of corresponding guide rail installations. Building on sensitivity analysis, some scholars have also researched tolerance design for critical geometric errors in machine tools. For instance, Cheng et al. (2018) calculated the first-order sensitivity and global sensitivity of geometric errors in CNC machine tools using the Sobol method. Specifically, they integrated sensitivity analysis results into the cost function for tolerance optimization design. Moreover, Wu et al. (2020a) traced 13 critical geometric errors in a three-axis CNC machine tool based on orthogonal experiments. By solving optimization objective functions, they provided tolerance bands for various critical errors under differing tolerance levels (IT2–IT10). Zhang et al. (2017) proposed an allocation approach of the geometric errors for optimizing total cost and reliability and used a mathematical model to perform the optimization process of accuracy allocation by using the non-dominated sorting genetic algorithm-II (NSGA-II).

Most of the research mentioned above uses sensitivity analysis to identify critical geometric errors, or key motion axes affecting machine tool machining accuracy, and provides guidance for accuracy allocation or geometric error compensation based on the results. In existing research, sensitivity analysis methods typically require measurement of all geometric errors of the machine tool, and the identification of critical errors is based on measured values (Xiang and Wu, 2021); this limits their effectiveness in guiding forward design of machine tools. In terms of guidance for machine tool accuracy allocation, most studies only determine key geometric error components (Chen et al., 2013; Cheng et al., 2014; Zhong et al., 2019; Fan et al., 2020; Niu et al., 2021), and methods that can quantitatively determine tolerance bandwidths for each error component are lacking (Cheng et al., 2014; Wu et al., 2020a). Furthermore, most studies focus on the positional deviations of machine tools, while neglecting tool direction deviations. In reality, five-axis machine tool direction deviations are of equal importance to positional deviations in many operating conditions (Xiong et al., 2019), such as drilling (Yuan et al., 2014; Lin et al., 2015), flank milling (Zhang et al., 2016), and gear form grinding (Xia et al., 2019, 2020).

To address the aforementioned issues, we propose an accuracy allocation method for five-axis machine tools based on geometric error sensitivity and cost analysis. The first step of the method is to allocate the allowable ranges of geometric error components that affect tool direction deviations, ensuring that the tool direction deviations at the sampling points meet the accuracy requirements. The next step is to allocate the allowable ranges of the remaining geometric error components, making sure that the positional deviations at the sampling points also meet the accuracy requirements. This approach ensures that both the positional and tool direction deviations are constrained. During the optimization process, it is objective that the cost sensitivities of each geometric error tend to be equal. This reasonably allocates costs to set tolerances for the geometric error components, resulting in the lowest-cost allocation scheme that meets the accuracy requirements.

2 Establishing the geometric error model

2.1 Sources of geometric errors in five-axis machine tools

According to the definition from ISO 230-1 (ISO, 2012a), each linear axis of a machine tool has six geometric errors. These include three linear errors in the directions of the three coordinate axes (one positioning error and two linear errors perpendicular to the axis) and three angular errors (the pitch, yaw, and roll errors). These geometric errors are related to the position of the motion axis and are called position-dependent geometric errors (PDGEs). They are primarily determined by the precision of the components that make up the motion axis. Additionally, there are three perpendicularity errors between the three linear axes, which are not related to the position of the motion axes. Such errors are called position-independent geometric errors (PIGEs), and are mainly caused by assembly deviations in the motion components. According to the definition in ISO 230-7 (ISO, 2012b), each machine tool rotary axis also has six PDGEs, comprising three linear errors and three angular errors. Additionally, each rotary axis has four PIGEs, including two perpendicularity errors and two positioning deviations in the direction perpendicular to the axis line. Fig. 1 shows the geometric errors described above, using the *Y*-axis and *C*-axis (a rotary axis) as an example.

2.2 Geometric error modeling of five-axis machine tools

Taking a typical BC-type (*B*-axis and *C*-axis type) five-axis machine tool with dual rotary tables as an

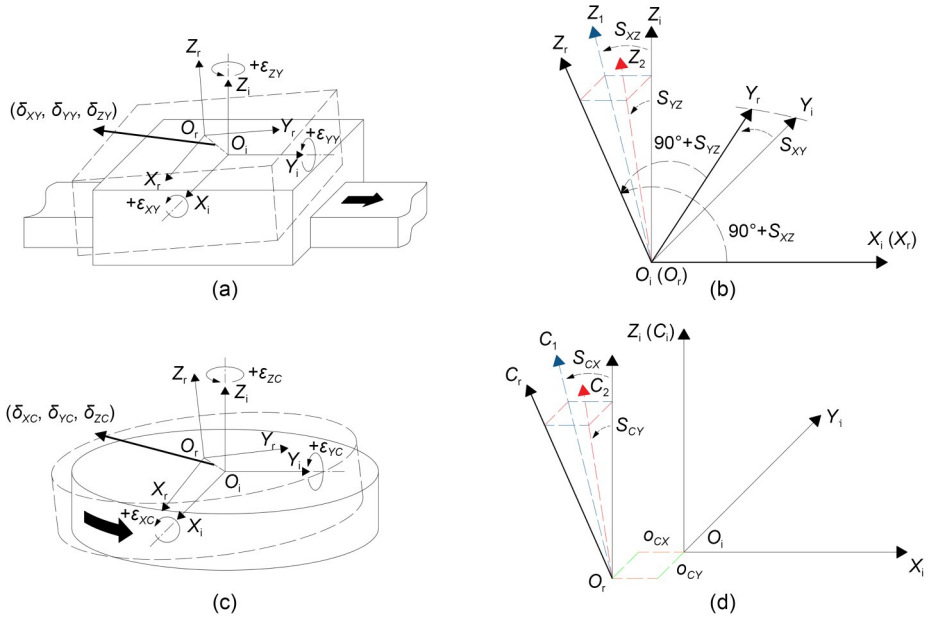

Fig. 1 Geometric errors in linear and rotary axes of a machine tool: (a) *Y*-axis PDGEs; (b) linear axis PIGEs; (c) *C*-axis PDGEs; (d) *C*-axis PIGEs. O_i-$X_iY_iZ_i$ is the ideal local coordinate system; O_r-$X_rY_rZ_r$ is the actual local coordinate system; other parameters are explained in the text and Table 1

example, we establish a geometric error model of the machine tool for subsequent sensitivity analysis. A schematic of the BC-type five-axis machine tool is shown in Fig. 2a, which includes three linear axes (*X*, *Y*, and *Z*) and two rotary axes (*B* and *C*). The kinematic chain of this machine tool is denoted as WCBMXYZT, and its kinematic chain structure is illustrated in Fig. 2b. Among the five axes, the *B*-axis and *C*-axis belong to the workpiece kinematic chain, while the *X*-axis, *Y*-axis, and *Z*-axis belong to the tool kinematic chain. The kinematic chain follows the transmission sequence of "WCS→CCS→BCS→MCS→XCS→YCS→ZCS→TCS". Here, WCS represents the workpiece coordinate system, and CCS, BCS, XCS, YCS, and ZCS represent the coordinate systems of the *C*-axis, *B*-axis, *X*-axis, *Y*-axis, and *Z*-axis, respectively. MCS represents the machine tool coordinate system, and TCS represents the tool coordinate system.

In the kinematic chain of the machine tool, there are a total of five motion components: the *X*, *Y*, *Z*, *B*, and *C* axes. As discussed earlier, these five motion axes involve a total of 41 geometric errors, including 30 PDGEs and 11 PIGEs. All the geometric errors are listed in Table 1, where δ represents linear error, ε represents angular error, *S* represents perpendicularity error, and *o* represents positioning deviation of the rotary axis in the direction perpendicular to the axis.

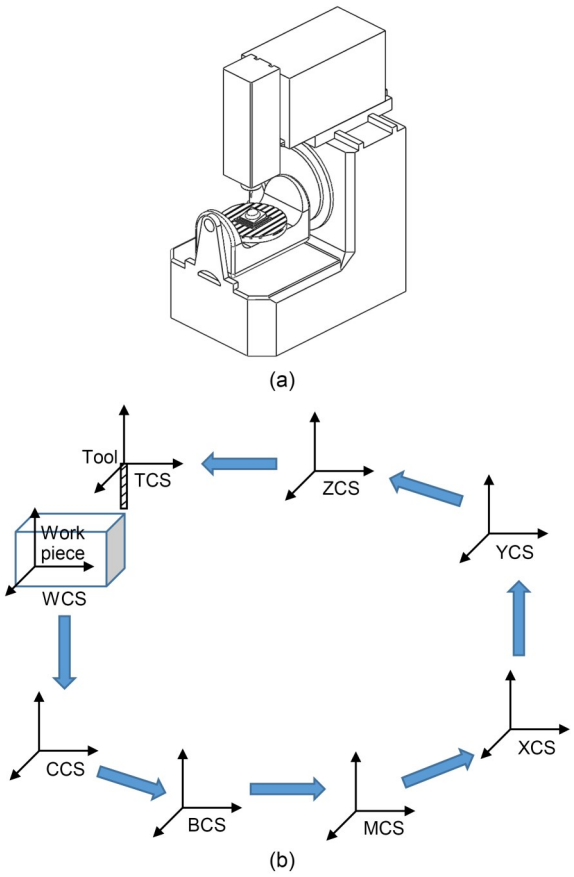

Fig. 2 Typical BC-type five-axis machine tool with dual rotary tables: (a) schematic diagram; (b) kinematic chain structure

Table 1 List of geometric errors for the BC-type five-axis machine tool with dual rotary tables

Item		Geometric error
PDGE	*X*-axis	δ_{XX}, δ_{YX}, δ_{ZX}, ε_{XX}, ε_{YX}, ε_{ZX}
	Y-axis	δ_{XY}, δ_{YY}, δ_{ZY}, ε_{XY}, ε_{YY}, ε_{ZY}
	Z-axis	δ_{XZ}, δ_{YZ}, δ_{ZZ}, ε_{XZ}, ε_{YZ}, ε_{ZZ}
	B-axis	δ_{XB}, δ_{YB}, δ_{ZB}, ε_{XB}, ε_{YB}, ε_{ZB}
	C-axis	δ_{XC}, δ_{YC}, δ_{ZC}, ε_{XC}, ε_{YC}, ε_{ZC}
PIGE		S_{XY}, S_{YZ}, S_{XZ}, S_{BX}, S_{BZ}, S_{CX}, S_{CY}, o_{BX}, o_{BZ}, o_{CX}, o_{CY}

In WCS, the error matrix *E* for tool positioning can be calculated as:

$$\boldsymbol{E} = {}^{\mathrm{T}}_{\mathrm{W}}\boldsymbol{T}^{\mathrm{r}} - {}^{\mathrm{T}}_{\mathrm{W}}\boldsymbol{T}^{\mathrm{i}}, \tag{1}$$

where ${}^{\mathrm{T}}_{\mathrm{W}}\boldsymbol{T}^{\mathrm{r}}$ is the actual transformation matrix from the tool coordinate system to the workpiece coordinate system, and ${}^{\mathrm{T}}_{\mathrm{W}}\boldsymbol{T}^{\mathrm{i}}$ is the ideal transformation matrix from the tool coordinate system to the workpiece coordinate system. Details of the model derivation are provided in the electronic supplementary materials (ESM).

3 Sensitivity and cost analyses of geometric errors over the volumetric workspace

3.1 Sensitivity analysis of geometric errors

We next conduct a sensitivity analysis to quantify the influence of each geometric error component (among the 41 input components) on the machine tool's positional and tool direction deviations. The Sobol method, which we will employ for this task, has two main characteristics (Wang et al., 2023): (1) it quantitatively analyzes the degree of influence of each input parameter on the model output; (2) it calculates the sensitivity index of each parameter within a specific range of values. In general, the geometric errors of machine tools are close to a normal distribution (Cheng et al., 2014). Therefore, in this study, all 41 geometric errors of the five-axis machine tool are considered as

normally distributed, with the center value μ being set to 0. Based on the basic rules of normal distributions, the relationship between the standard deviation σ and the tolerance bandwidth T is $T=6\sigma$ (Wu et al., 2020b). Points were randomly sampled within the normal distribution range of the 41 geometric errors using the Sobol sequence method (Sobol, 2001), which has high stability and fast convergence. Then, the Saltelli sampling method (Chan et al., 1997) was used to construct a sample list and a corresponding model output list, based on which the Sobol indices of the model inputs were calculated. Compared to the original Sobol method, the Saltelli sampling method has a smaller computational load and is easier to implement in programming.

3.2 Volumetric sampling points considering the tool direction deviation

The input for the geometric error model consists of 41 geometric error values and a five-axis coordinate point P. Therefore, a single Sobol sensitivity analysis can only yield sensitivity indices for the 41 geometric errors at a single five-axis coordinate point P, i.e., ${}^{P}S_i\,(i=1,\ 2,\ \cdots,\ 41)$. These sensitivity indices represent the importance of each geometric error in influencing the machine tool's positional or tool direction deviation at that point. To ensure that the sensitivity analysis results reflect the characteristics of geometric errors in the workspace of the machine tool, a sensitivity analysis for geometric errors in the workspace of the machine tool is proposed.

As shown in Fig. 3, n sampling points are selected symmetrically at the centers of four body diagonals in the workspace of the machine tool's linear axes, resulting in a total of $4n$ thee-axis coordinates. Then, within the stroke ranges of the two rotary axes of the machine tool, m_1 and m_2 sampling points are selected. By combining the sampling points of the linear and rotary axes, a total of $4nm_1m_2$ five-axis coordinates $P_j\,(j=1,\ 2,\ \cdots,\ 4nm_1m_2)$ can be obtained. This list of five-axis coordinates provides the sampling points for subsequent sensitivity analysis of the workspace, and the development of precision equivalence algorithms.

The selection of sampling points is based on actual operating conditions. As such, the points are not evenly distributed considering the frequency distribution of the linear and rotary axes. We found that the results of the sensitivity analysis based on the volumetric sampling points shown in Fig. 3 are relatively close

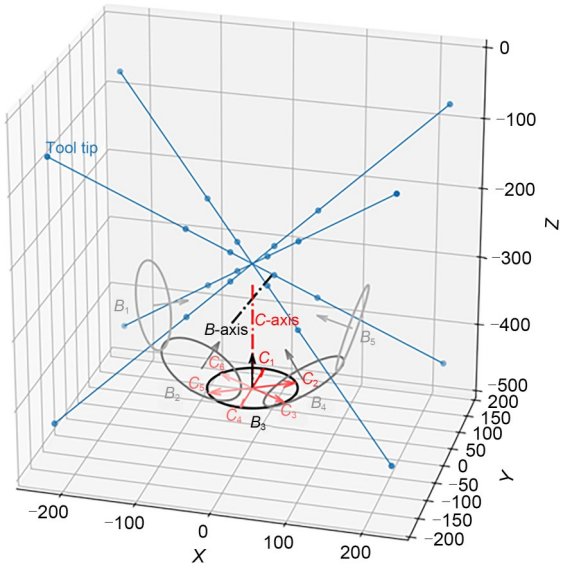

Fig. 3 Volumetric sampling points from a combination of the linear and rotary axes

to those based on the tool paths of specific workpieces. Therefore, these volumetric sampling points can be used as a basis for general analysis.

By performing a single Sobol sensitivity analysis for the positional and tool direction deviations at each sampling point P_j, sensitivity indices ${}^{P_j}S_i\,(i=1,\ 2,\ \cdots,\ 41;j=1,\ 2,\ \cdots,\ 4nm_1m_2)$ for the 41 geometric errors can be obtained. In this study, the sensitivity indices of the geometric errors at all sampling points are averaged, to obtain the sensitivity indices for the machine tool's workspace:

$$S_i^{\mathrm{T}}=\frac{1}{4nm_1m_2}\sum_{j=1}^{4nm_1m_2}{}^{P_j}S_i. \tag{2}$$

This sensitivity index S_i^{T} represents the importance of each geometric error in influencing the overall positional deviation or tool direction deviation of the machine tool. A higher sensitivity index for a certain geometric error indicates that this geometric error is more impactful on the positional deviation or tool direction deviation.

3.3 Geometric error cost sensitivity

The sensitivity analysis in Section 3.1 indicates which error components are more important, but it ignores the manufacturing cost of each error component. A cost analysis is necessary to determine which error components can reasonably be addressed.

Therefore, we conduct a cost analysis of the geometric errors based on a cost tolerance model. According to relevant literature (Armillotta, 2020), commonly used cost tolerance models comprise 13 types, such as the exponential model, reciprocal model, reciprocal square model, reciprocal power model, and polynomial model. Among these, the reciprocal square model is most commonly used:

$$c(T)=a+\frac{b}{T^2}, \tag{3}$$

where c represents the part manufacturing cost, T represents the tolerance, a represents a fixed cost constant that is independent of the tolerance, and b represents the coefficient of the feature curve related to the tolerance. Considering how the geometric errors of each axis accumulate (due to the manufacturing and assembly tolerances of the components of each axis), we choose to substitute the tolerance bandwidth of the geometric error components in the reciprocal square model to calculate the cost; this represents the estimated cost of controlling the tolerance bandwidth of the geometric error components. In this case, the estimated cost of the overall machine accuracy design can be represented as:

$$c_{\text{total}}=\sum_{i=1}^{41}c(T_i)=\sum_{i=1}^{41}\frac{k_i}{T_i^2}, \tag{4}$$

where c_{total} is the total estimated cost of the machine accuracy design, T_i represents the allowable range of variation for the ith geometric error, and k_i represents the cost coefficient of the ith geometric error. Since different geometric error components have different impacts on the overall machine accuracy, as well as varying implementation difficulties (Tian, 2014), their differences in sensitivity and implementation cost should be considered when allocating the allowable variation ranges. The cost coefficient k_i of the geometric error components represents the difficulty of achieving static accuracy for that geometric error component, including both PDGEs and PIGEs. This coefficient can be determined through regression analysis based on relevant data held by the machine tool manufacturer.

Considering how the sensitivities of the geometric error components represent their impact on overall accuracy, we want to allocate more cost to the important error components and avoid wasting cost on noncritical error components. Accordingly, we propose using the ratio of the sensitivity of the geometric error components to their estimated cost as the cost sensitivity, that is:

$$\omega_i=\frac{S_i^{\mathrm{T}}}{c_i}, \tag{5}$$

where ω_i represents the cost sensitivity of the ith geometric error component, S_i^{T} represents its sensitivity index, and c_i represents its estimated cost. The cost sensitivity of a geometric error component essentially expresses the impact of cost changes on accuracy for that specific component. When the sensitivity of a geometric error component is low and the implementation cost is high, the cost sensitivity of that geometric error component is low, indicating that cost changes have a limited impact on accuracy, and implying a significant waste of funds; in this case, the tolerance level for that geometric error component should be relaxed. Conversely, when the sensitivity of a geometric error component is high and the implementation cost is low, it indicates that cost changes can effectively improve the accuracy. In this scenario, there is still room for improvement in the accuracy of that geometric error component, and it is recommended to increase the cost invested into that geometric error component and reduce the tolerance.

Under this assumption, when the cost sensitivities of each geometric error component in an accuracy allocation scheme are equal, it indicates that the cost of the precision design is optimally utilized across all components. Such an allocation scheme is considered to have the lowest cost.

4 Accuracy allocation with priority given to tool direction deviation

4.1 Priority of tool direction deviation and angular error components

As stated in Section 1, the issue of tool direction deviation is neglected in most studies despite its importance (Xiong et al., 2019), particularly for situations such as drilling (Yuan et al., 2014; Lin et al., 2015), flank milling (Zhang et al., 2016), and gear form grinding (Xia et al., 2019, 2020). In the conditions above,

tool direction deviation impacts the resulting quality of the target surface, for instance in regard to the perpendicularity of the central axis of a drilled hole, the parallelism and perpendicularity of a milled side, or the precision of a gear surface. Thus, only ensuring positional precision may mean that geometric dimensioning and tolerancing (GD&T) requirements are not met.

Here, we elaborate on this point for the situation of flank milling. As shown in Fig. S1a of the ESM, an inclined conical workpiece is being processed by five-axis flank milling, whose GD&T requirements are given by the surface profile in Fig. S1b. Fig. S1c shows both the ideal condition and the condition where there is a tool direction deviation ($\Delta \boldsymbol{V}$). The point at the tip of the tool is controlled to ensure positional precision in both conditions. However, as shown in Fig. S1d, the tool direction deviation may cause the inclined cone surface profile to fail to meet the GD&T requirements.

In conditions with stringent GD&T requirements, positional precision control alone may be insufficient to meet the requirements. Thus, tool direction deviation should also be considered.

Among all 41 error components, the linear error components can only affect the positional deviation. Only angular error components can affect tool direction deviation, and they also affect positional deviation. Depending on the geometric model for each machine tool, some of the angular error components whose rotation vector is parallel to the tool vector do not affect tool direction deviation, either. Therefore, we propose a method of first adjusting error components that affect tool direction deviation, and then adjusting the remaining error components to ensure that the allocation scheme meets the requirements for both tool direction and positional deviations. The first stage of adjustment only adjusts those error components affecting the tool direction deviation, making sure that the tool direction deviation meets the requirements. In the first stage of adjustment, error components with zero sensitivity to tool direction deviation are ignored, and their value ranges will be determined in the second stage of adjustment. The second stage of adjustment will start only when all value ranges of error components affecting tool direction deviation have been determined. Through the above method, both tool direction and positional deviations of the machine tool can be controlled.

4.2 Accuracy allocation process

During the adjustment of the tolerance bandwidths for various geometric error components, it is essential to ensure that each iteration scheme possesses equivalent accuracy. In other words, the tool direction deviation $\Delta \boldsymbol{V}$ and the positional deviation $\Delta \boldsymbol{P}$ for each iteration scheme should be at similar levels. Therefore, we constrain the machine tool's directional and positional deviations by probabilities of $\Delta \boldsymbol{V}$ and $\Delta \boldsymbol{P}$, respectively, to be less than a certain threshold at any five-axis coordinates. The range of percentages these probabilities fall into will define the target accuracy of the machine tool.

In this study, we use a globally scaled accuracy allocation scheme called the overall scaling algorithm, as depicted in Fig. 4a. This ensures that both the initially determined tolerance allocations and each set of accuracy allocation schemes meet the accuracy criteria during the iterative process, thus enabling precision equivalence.

Based on the previous analysis, we know that the cost sensitivity index represents the impact of the cost change of geometric error components on the machine tool accuracy. When the cost sensitivities of each geometric error component are equalized, the accuracy allocation scheme with the lowest cost is achieved. Meanwhile, considering that the tool direction deviation $\Delta \boldsymbol{V}$ is only influenced by angular error components, the geometric error components affecting $\Delta \boldsymbol{V}$ are allocated first in the adjustment to achieve the target directional precision. Subsequently, the remaining geometric error components are allocated to achieve the target positional precision. The adjustment algorithm proposed in this study can be summarized as follows:

Step 1. Use the global scaling algorithm to scale the initially determined tolerance values for the 41 geometric error components, achieving the target precision. Then, output the scaled accuracy allocation scheme A_1 as the initial value for optimization.

Step 2. Perform sensitivity analysis on the scaled tolerance values, calculating the cost sensitivity index ω_i.

Step 3. Calculate the average value of cost sensitivity for each geometric error component, i.e., $\bar{\omega} = \frac{1}{n}\sum_{i=1}^{n}\omega_i$, and adjust the tolerance of each geometric error component using the difference $(\omega_i - \bar{\omega})$ as feedback, i.e., $T_i^j = k\,(\omega_i - \bar{\omega})\,T_i^{j-1}$.

Step 4. Use the global scaling algorithm on the adjusted tolerance values T_i^j to achieve the target

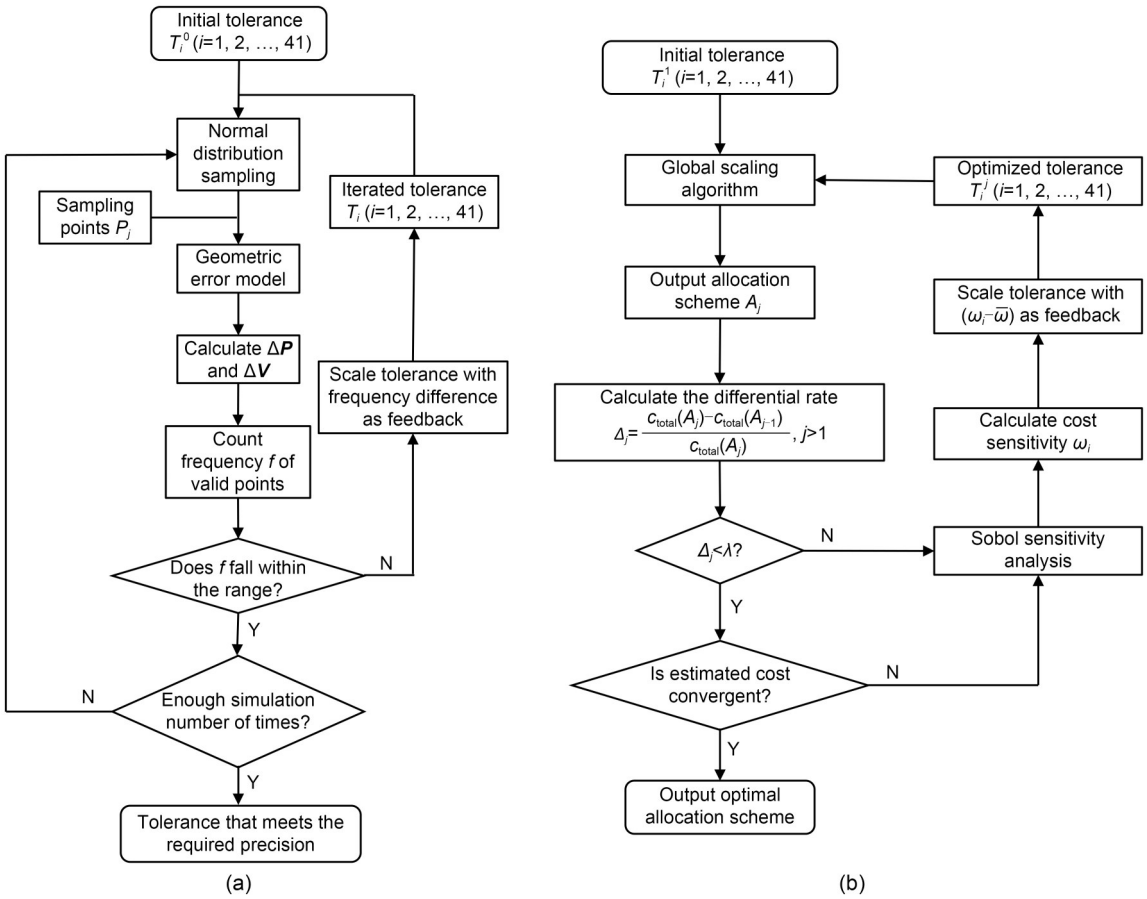

Fig. 4 Accuracy allocation process: (a) global scaling algorithm for precision equivalence; (b) accuracy allocation process based on equivalent geometric error cost sensitivities

precision. Then, output the scaled accuracy allocation scheme A_j as the iterated result.

Step 5. Calculate the differential rate Δ_j of the estimated cost between two iterations. If Δ_j is less than a specific threshold λ in consecutive iterations, it indicates that the estimated cost is convergent, and the allocation scheme can be selected as the final output. Otherwise, repeat Step 2 iteratively.

A flowchart of the algorithm is shown in Fig. 4b.

5 Simulation and verification

5.1 Configuration of initial parameters

The BC-type five-axis machine tool with dual rotary tables shown in Fig. 2 is next used to conduct a simulation. Based on the theory of homogeneous transform matrix (HTM), we calculated the coordinate transformation matrices between each coordinate system. We used the Python programming language to establish the geometric error model of the machine tool, enabling the calculation of positional deviation $\Delta\boldsymbol{P}$ and tool direction deviation $\Delta\boldsymbol{V}$.

In the simulation, six test points were selected along the four body diagonals within the workspace of three linear axes of the machine tool, as shown in Fig. 3. The distribution of sampling points for the rotary axes is presented in Table 2. After permutation and combination, a total of 720 sampling points were generated over the volumetric workspace.

Table 2 Distribution of sampling points for rotary axes

Rotary axis	Sampling position
B-axis	−75°, −30°, 0°, 30°, 75°
C-axis	0°, 60°, 120°, 180°, 240°, 300°

Initial tolerance ranges for the 41 geometric errors were set based on achievable accuracies for typical five-axis CNC machine tools and some relevant references (Cheng et al., 2014). Among them, the tolerance

range for 19 linear errors was set to [−10, 10] μm, and the tolerance range for 22 angular errors was set to [−20, 20] μrad.

Based on relevant design requirements suggested in the literature, we set the accuracy thresholds for positional deviation and tool direction deviation to be 20 μm and 40 μrad, respectively. We also set the specific percentage range (described in Section 4.2) to be (95±1)%. This means the probability that $|\Delta \boldsymbol{V}| \leqslant 40$ μrad and $|\Delta \boldsymbol{P}| \leqslant 20$ μm at any five-axis coordinate should be within the range of (95±1)% in order to meet the target accuracy.

5.2 Tool direction accuracy allocation

The precision-equivalent scaling algorithm shown in Fig. 4a was used on the initial tolerance values to adjust the angular error components that affect tool direction deviation. This adjustment was made to ensure that the tool direction deviation from the tolerance configuration met the target accuracy. The scaled tolerance configuration was then used as the initial value in the optimization, as shown in Table 3.

To achieve the target accuracy for tool direction deviation, among the 22 angular error components, the allowable range for 17 components was reduced from the initial [−20, 20] μrad to [−18.2, 18.2] μrad. However, five angular error components, ε_{ZX}, ε_{ZY}, ε_{ZZ}, S_{XY}, and S_{BX}, remained unchanged. This is because the vectors of these components are parallel to the tool axis and do not affect the tool direction deviation. Additionally, two angle error components, ε_{ZY} and ε_{ZZ}, coincide with the tool axis and therefore do not affect the positional deviation. Hence, the actual number of error components that need to be allocated is 39. The sensitivity analysis for tool direction deviation based on the initial tolerance configuration is shown in Fig. 5.

In the simulation, the inverse square cost tolerance model was used to calculate the cost of the geometric error components, as shown in Eq. (4). Generally, it is more challenging to control PDGEs in linear axes than in rotational axes, and PIGEs tend to be much larger than PDGEs (Chen et al., 2023). Therefore, we assigned coefficient values of 1.0, 0.5, and 4.0 to the cost tolerance model for PDGEs in linear axes, PDGEs in rotational axes, and PIGEs, respectively. The initial values, as shown in Table 3, were optimized using the aforementioned accuracy allocation method. The iterative process is depicted in Fig. 6a, and the sensitivity analysis results after convergence are shown in Fig. 6b. The geometric error components that underwent changes are listed in Table 4. From Fig. 6a, one can observe that the result converges after approximately eight iterations. Fig. 6b reveals that the cost sensitivities of various error components become approximately equal after optimization, indicating that the cost has been maximally utilized (i.e., the resulting allocation plan is the one with the lowest cost). If we only consider the error components involved in the adjustment, then

Table 3 Optimization initial values (unit: μm for linear error component; μrad for angular error component)

Error item	Allowable range	Error item	Allowable range	Error item	Allowable range
δ_{XX}	[−10.0, 10.0]	δ_{ZZ}	[−10.0, 10.0]	$^{*}\varepsilon_{YC}$	[−18.2, 18.2]
δ_{YX}	[−10.0, 10.0]	$^{*}\varepsilon_{XZ}$	[−18.2, 18.2]	$^{*}\varepsilon_{ZC}$	[−18.2, 18.2]
δ_{ZX}	[−10.0, 10.0]	$^{*}\varepsilon_{YZ}$	[−18.2, 18.2]	S_{XY}	[−20.0, 20.0]
$^{*}\varepsilon_{XX}$	[−18.2, 18.2]	ε_{ZZ}	[−20.0, 20.0]	$^{*}S_{YZ}$	[−18.2, 18.2]
$^{*}\varepsilon_{YX}$	[−18.2, 18.2]	δ_{XB}	[−10.0, 10.0]	$^{*}S_{XZ}$	[−18.2, 18.2]
ε_{ZX}	[−20.0, 20.0]	δ_{YB}	[−10.0, 10.0]	S_{BX}	[−20.0, 20.0]
δ_{XY}	[−10.0, 10.0]	δ_{ZB}	[−10.0, 10.0]	$^{*}S_{BZ}$	[−18.2, 18.2]
δ_{YY}	[−10.0, 10.0]	$^{*}\varepsilon_{XB}$	[−18.2, 18.2]	$^{*}S_{CX}$	[−18.2, 18.2]
δ_{ZY}	[−10.0, 10.0]	$^{*}\varepsilon_{YB}$	[−18.2, 18.2]	$^{*}S_{CY}$	[−18.2, 18.2]
$^{*}\varepsilon_{XY}$	[−18.2, 18.2]	$^{*}\varepsilon_{ZB}$	[−18.2, 18.2]	o_{BX}	[−10.0, 10.0]
$^{*}\varepsilon_{YY}$	[−18.2, 18.2]	δ_{XC}	[−10.0, 10.0]	o_{BZ}	[−10.0, 10.0]
ε_{ZY}	[−20.0, 20.0]	δ_{YC}	[−10.0, 10.0]	o_{CX}	[−10.0, 10.0]
δ_{XZ}	[−10.0, 10.0]	δ_{ZC}	[−10.0, 10.0]	o_{CY}	[−10.0, 10.0]
δ_{YZ}	[−10.0, 10.0]	$^{*}\varepsilon_{XC}$	[−18.2, 18.2]		

* indicates variations in error components. Total estimated cost only considering the error components with variations: $c_{\text{total}} = \sum_{i=1}^{18} c(T_i) = \sum_{i=1}^{18} \frac{k_i}{T_i^2} = 8774669$

during the allocation of angular error components affecting tool direction deviation, the geometric error cost decreased by 15.2%.

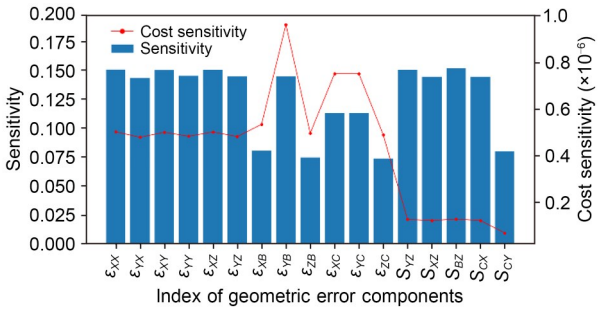

Fig. 5 Sensitivity analysis of tool direction deviation for the initial tolerance values

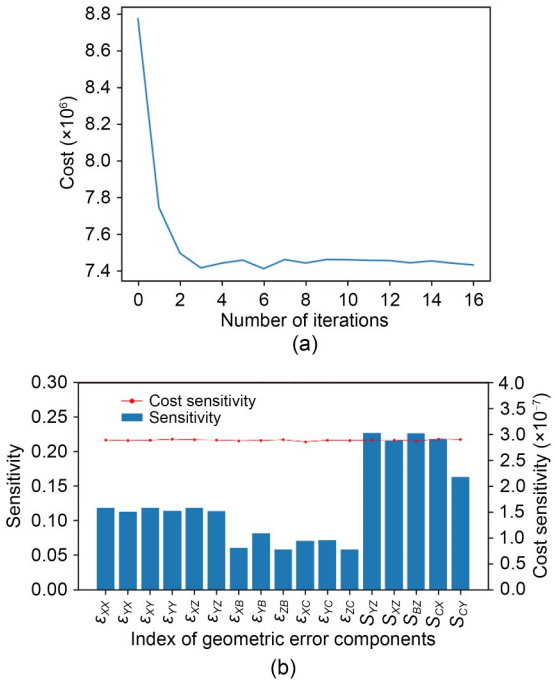

Fig. 6 Optimization results of tool directional deviation: (a) iterative optimization process; (b) sensitivity analysis results after convergence

5.3 Positional accuracy allocation

In Section 5.2, the allowable ranges of 17 angular error components were determined to ensure that the tool direction deviation reached the target accuracy. Subsequently, the remaining 22 geometric error components were allocated to achieve the target accuracy for positional deviation. The precision-equivalent scaling algorithm shown in Fig. 4a was applied to the optimized allocation scheme (described in Section 5.2) to scale the remaining 22 geometric error components, ensuring that the positional deviation in the tolerance configuration met the target accuracy. The geometric error components that underwent changes are listed in Table 5, and were used as the initial values for positional deviation optimization. Sensitivity analysis for positional deviation based on the initial tolerance configuration is shown in Fig. 7. Following the same accuracy allocation method, the remaining 22 geometric error components were iteratively optimized. The process is shown in Fig. 8a, the sensitivity analysis results after convergence are presented in Fig. 8b, and the optimization results are summarized in Table 6. Solely considering the error components involved in the adjustment, during the optimization of the positional deviation, the geometric error cost decreased by 34.4%.

5.4 Allocation results and verification

In the two adjustment iterations, the cost sensitivities of the geometric error components involved in the adjustments tended to be equal, and both the tool direction and positional deviations reached the target precision, indicating that the method converged. The accuracy allocation scheme, as shown in Tables 4 and 6, includes the allowable ranges of all geometric error components that need to be determined. From Tables 4 and 6, it can be determined that the total estimated cost of the allocation scheme is 15163102.

Table 4 Geometric error components with variations during tool direction deviation optimization (unit: μrad)

Error item	Allowable range	Error item	Allowable range	Error item	Allowable range
ε_{XX}	[−15.6, 15.6]	ε_{XB}	[−15.4, 15.4]	S_{YZ}	[−22.6, 22.6]
ε_{YX}	[−15.9, 15.9]	ε_{YB}	[−13.3, 13.3]	S_{XZ}	[−23.2, 23.2]
ε_{XY}	[−15.6, 15.6]	ε_{ZB}	[−15.7, 15.7]	S_{BZ}	[−22.5, 22.5]
ε_{YY}	[−15.9, 15.9]	ε_{XC}	[−14.2, 14.2]	S_{CX}	[−23.1, 23.1]
ε_{XZ}	[−15.6, 15.6]	ε_{YC}	[−14.1, 14.1]	S_{CY}	[−26.7, 26.7]
ε_{YZ}	[−15.9, 15.9]	ε_{ZC}	[−15.7, 15.7]		

Total estimated cost only considering the error components above: $c_{\text{total}} = \sum_{i=1}^{18} c(T_i) = \sum_{i=1}^{18} \frac{k_i}{T_i^2} = 7442521$

Table 5 Initial values for positional deviation optimization (unit: μm for linear error component; μrad for angular error component)

Error item	Allowable range	Error item	Allowable range	Error item	Allowable range
δ_{XX}	[−7.56, 7.56]	δ_{YZ}	[−7.56, 7.56]	S_{XY}	[−15.1, 15.1]
δ_{YX}	[−7.56, 7.56]	δ_{ZZ}	[−7.56, 7.56]	S_{BX}	[−15.1, 15.1]
δ_{ZX}	[−7.56, 7.56]	δ_{XB}	[−7.56, 7.56]	o_{BX}	[−7.56, 7.56]
ε_{ZX}	[−15.1, 15.1]	δ_{YB}	[−7.56, 7.56]	o_{BZ}	[−7.56, 7.56]
δ_{XY}	[−7.56, 7.56]	δ_{ZB}	[−7.56, 7.56]	o_{CX}	[−7.56, 7.56]
δ_{YY}	[−7.56, 7.56]	δ_{XC}	[−7.56, 7.56]	o_{CY}	[−7.56, 7.56]
δ_{ZY}	[−7.56, 7.56]	δ_{YC}	[−7.56, 7.56]		
δ_{XZ}	[−7.56, 7.56]	δ_{ZC}	[−7.56, 7.56]		

Total estimated cost only considering the error components above: $c_{\text{total}} = \sum_{i=1}^{21} c(T_i) = \sum_{i=1}^{21} \frac{k_i}{T_i^2} = 11778153$

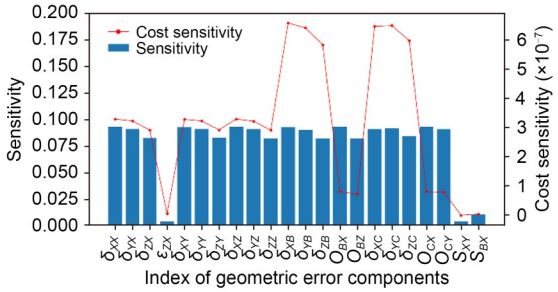

Fig. 7 Sensitivity analysis of positional deviation for initial tolerance values

A uniform allocation scheme was used for comparison with our allocation method. Essentially, a distribution scheme with the uniform allocation of linear and angular errors is used to achieve the same target precision, with the resulting geometric error tolerance list shown in Table 7.

The simulation results indicate that compared to the uniform allocation scheme, our accuracy allocation scheme reduces the overall geometric error estimated cost by 27.8% (from 20997862 to 15163102) while maintaining the target precision for both tool direction and positional deviations.

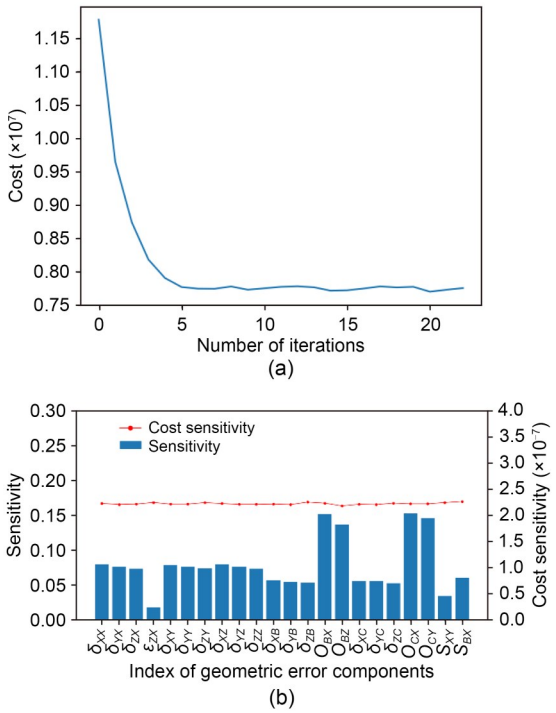

Fig. 8 Optimization results of positional deviation: (a) iterative optimization process; (b) sensitivity analysis results after convergence

Table 6 Final values of positional deviation optimization (unit: μm for linear error component; μrad for angular error component)

Error item	Allowable range	Error item	Allowable range	Error item	Allowable range
δ_{XX}	[−6.71, 6.71]	δ_{YZ}	[−6.81, 6.81]	S_{XY}	[−51.2, 51.2]
δ_{YX}	[−6.80, 6.80]	δ_{ZZ}	[−6.95, 6.95]	S_{BX}	[−38.7, 38.7]
δ_{ZX}	[−6.95, 6.95]	δ_{XB}	[−5.59, 5.59]	o_{BX}	[−9.70, 9.70]
ε_{ZX}	[−35.9, 35.9]	δ_{YB}	[−5.69, 5.69]	o_{BZ}	[−10.11, 10.11]
δ_{XY}	[−6.71, 6.71]	δ_{ZB}	[−5.84, 5.84]	o_{CX}	[−9.65, 9.65]
δ_{YY}	[−6.81, 6.81]	δ_{XC}	[−5.63, 5.63]	o_{CY}	[−9.86, 9.86]
δ_{ZY}	[−6.95, 6.95]	δ_{YC}	[−5.64, 5.64]		
δ_{XZ}	[−6.71, 6.71]	δ_{ZC}	[−5.83, 5.83]		

Total estimated cost only considering the error components above: $c_{\text{total}} = \sum_{i=1}^{21} c(T_i) = \sum_{i=1}^{21} \frac{k_i}{T_i^2} = 7720581$

Table 7 Uniform allocation scheme (unit: μm for linear error component; μrad for angular error component)

Error item	Allowable range	Error item	Allowable range	Error item	Allowable range
δ_{XX}	[−7.42, 7.42]	δ_{ZZ}	[−7.42, 7.42]	ε_{YC}	[−18.2, 18.2]
δ_{YX}	[−7.42, 7.42]	ε_{XZ}	[−18.2, 18.2]	ε_{ZC}	[−18.2, 18.2]
δ_{ZX}	[−7.42, 7.42]	ε_{YZ}	[−18.2, 18.2]	S_{XY}	[−14.8, 14.8]
ε_{XX}	[−18.2, 18.2]	ε_{ZZ}	[−20.0, 20.0]	S_{YZ}	[−18.2, 18.2]
ε_{YX}	[−18.2, 18.2]	δ_{XB}	[−7.42, 7.42]	S_{XZ}	[−18.2, 18.2]
ε_{ZX}	[−14.8, 14.8]	δ_{YB}	[−7.42, 7.42]	S_{BX}	[−14.8, 14.8]
δ_{XY}	[−7.42, 7.42]	δ_{ZB}	[−7.42, 7.42]	S_{BZ}	[−18.2, 18.2]
δ_{YY}	[−7.42, 7.42]	ε_{XB}	[−18.2, 18.2]	S_{CX}	[−18.2, 18.2]
δ_{ZY}	[−7.42, 7.42]	ε_{YB}	[−18.2, 18.2]	S_{CY}	[−18.2, 18.2]
ε_{XY}	[−18.2, 18.2]	ε_{ZB}	[−18.2, 18.2]	o_{BX}	[−7.42, 7.42]
ε_{YY}	[−18.2, 18.2]	δ_{XC}	[−7.42, 7.42]	o_{BZ}	[−7.42, 7.42]
ε_{ZY}	[−20.0, 20.0]	δ_{YC}	[−7.42, 7.42]	o_{CX}	[−7.42, 7.42]
δ_{XZ}	[−7.42, 7.42]	δ_{ZC}	[−7.42, 7.42]	o_{CY}	[−7.42, 7.42]
δ_{YZ}	[−7.42, 7.42]	ε_{XC}	[−18.2, 18.2]		

Total estimated cost: $c_{\text{total}}=\sum_{i=1}^{39}c(T_i)=\sum_{i=1}^{39}\frac{k_i}{T_i^2}=20997862$

A total of 10000 random sampling points were selected in a uniform distribution across the machine tool's workspace along each axis. The number and frequency (percentage) of points satisfying $|\Delta \boldsymbol{V}|\leqslant$ 40 μrad for tool direction deviation and $|\Delta \boldsymbol{P}|\leqslant$20 μm for positional deviation were counted under the accuracy allocation. The results are presented in Table 8, showing that the frequencies fall within the interval of (95±1)%. This indicates that the allocation scheme meets the previously mentioned target precisions for both positional and tool direction deviations.

Table 8 Deviation statistics of randomly sampled points (10000 points) within the workspace

Item	Quantity of satisfying points	Frequency of satisfying points (%)
$|\Delta \boldsymbol{V}|\leqslant$40 μrad	9550	95.50
$|\Delta \boldsymbol{P}|\leqslant$20 μm	9416	94.16

Using both the uniform allocation scheme shown in Table 7 and the proposed accuracy allocation scheme, simulations were conducted for machining an inclined conical part, as shown in Fig. 9. The simulation results are presented in Fig. 10, Fig. 11, and Table 9. Figs. 10a and 10b represent the positional deviations of both allocation schemes. Figs. 11a and 11b represent the tool direction deviations of both allocation schemes. One can see that both allocation schemes yield the same accuracy. From Table 9, it is clear that our proposed method achieves a reduction in geometric error cost while maintaining the overall precision of the machine tool.

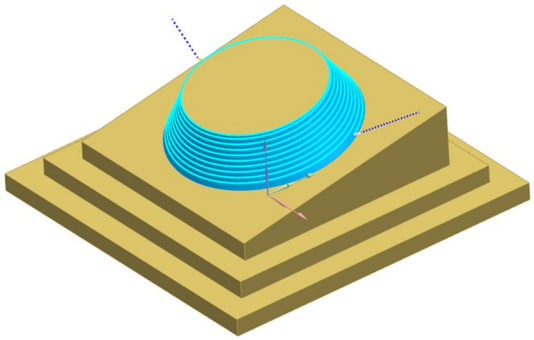

Fig. 9 Inclined conical workpiece

5.5 Verification of priority for tool direction deviation

To verify the sequence of adjusting the error components does indeed impact the allocation results, a comparative simulation was conducted; specifically, the error components that do not affect tool direction deviation are allocated first and those that do are allocated second. That is to say, the positional accuracy is allocated first while the tool direction accuracy is allocated second. This is the opposite of our proposed method. The two-step allocation results are listed in Tables 10 and 11.

From Tables 6 and 10, one can observe that the sequence of adjusting the error components indeed affects the allocation results, which is reflected in how all the error components are allocated to narrower allowable ranges (Table 10). Thus, the total estimated cost has increased from 7720581 to 8603772. However, looking at Tables 4 and 11, the results are almost unchanged.

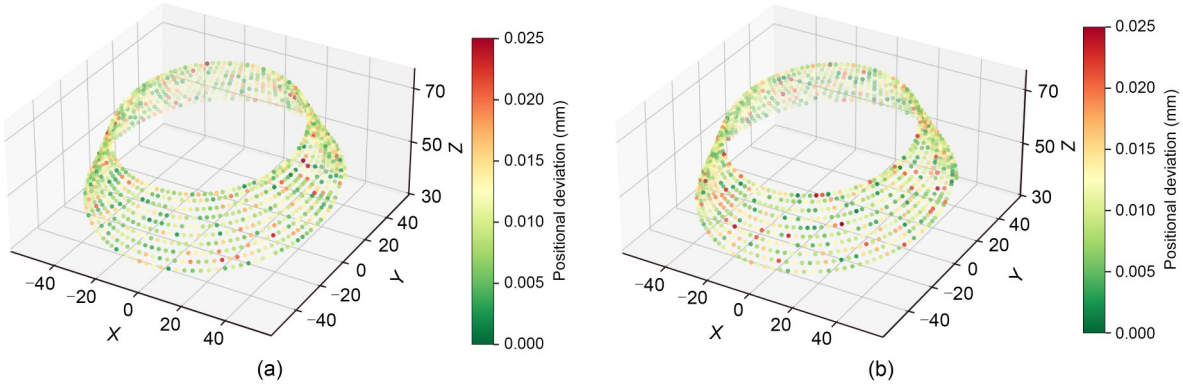

Fig. 10 Simulated machining results of positional deviation: (a) proposed allocating scheme; (b) uniform allocation scheme

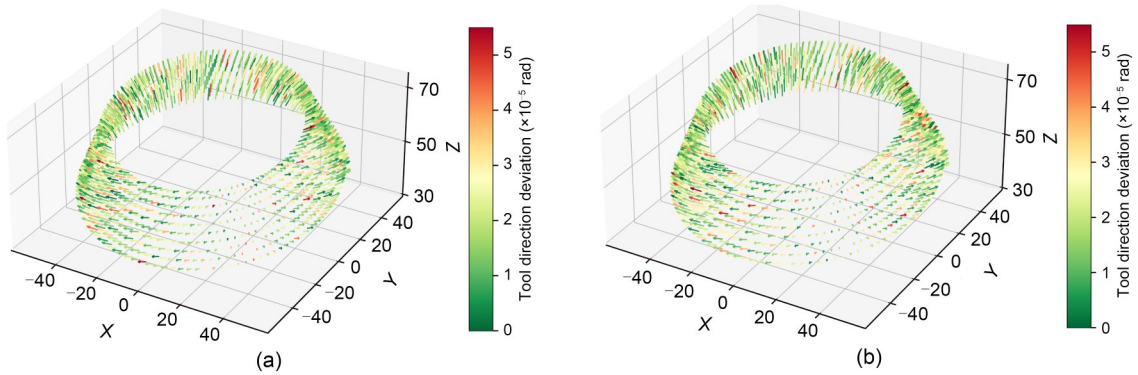

Fig. 11 Simulated machining results of tool direction deviation: (a) proposed allocating scheme; (b) uniform allocation scheme

Table 9 Comparison of simulated machining results

Parameter	Value		Improvement rate
	Uniform allocation scheme	Proposed allocation scheme	
Mean positional deviation (mm)	0.0108	0.0107	−0.93%
Variance of positional deviation (mm^2)	2.04×10^{-5}	1.94×10^{-5}	–
Frequency of $\lvert\Delta\boldsymbol{P}\rvert\leqslant20$ μm	0.9688	0.9696	+0.08%
Mean tool direction deviation (rad)	2.00×10^{-5}	1.99×10^{-5}	−0.50%
Variance of tool direction deviation (rad^2)	1.08×10^{-10}	1.15×10^{-10}	–
Frequency of $\lvert\Delta\boldsymbol{V}\rvert\leqslant40$ μrad	0.9584	0.9592	+0.08%
Estimated cost	20997862	15163102	−27.8%

The effects of the adjusting sequence and the difference between the two types of error components can be explained by the following: when allocating positional accuracy in the comparative simulation, each error component affecting tool direction deviation remained at its original standard [−20, 20] μrad, which could not meet the tool direction accuracy requirement. However, when allocating positional accuracy in the formal experiment, the directional accuracy had already been allocated, and the error components affecting tool direction deviation were adjusted to a higher precision standard than [−20, 20] μrad. Thus, in the comparative simulation, the error components in Table 10 had to be adjusted to narrower allowable ranges to compensate for the differences in angular error components. For both the formal and comparative simulations, the process for directional accuracy allocation involved the same input, and hence there are limited differences between the results shown in Tables 4 and 11.

Table 10 Final values of positional deviation optimization (unit: μm for linear error component; μrad for angular error component)

Error item	Allowable range	Error item	Allowable range	Error item	Allowable range
δ_{XX}	[−6.34, 6.34]	δ_{YZ}	[−6.42, 6.42]	S_{XY}	[−48.7, 48.7]
δ_{YX}	[−6.42, 6.42]	δ_{ZZ}	[−6.65, 6.65]	S_{BX}	[−36.7, 36.7]
δ_{ZX}	[−6.64, 6.64]	δ_{XB}	[−5.32, 5.32]	o_{BX}	[−9.12, 9.12]
ε_{ZX}	[−34.1, 34.1]	δ_{YB}	[−5.36, 5.36]	o_{BZ}	[−9.68, 9.68]
δ_{XY}	[−6.33, 6.33]	δ_{ZB}	[−5.54, 5.54]	o_{CX}	[−9.16, 9.16]
δ_{YY}	[−6.42, 6.42]	δ_{XC}	[−5.34, 5.34]	o_{CY}	[−9.26, 9.26]
δ_{ZY}	[−6.66, 6.66]	δ_{YC}	[−5.35, 5.35]		
δ_{XZ}	[−6.33, 6.33]	δ_{ZC}	[−5.54, 5.54]		

Total estimated cost only considering the error components above: $c_{\text{total}}=\sum_{i=1}^{21}c(T_i)=\sum_{i=1}^{21}\frac{k_i}{T_i^2}=8603772$

Table 11 Final values of tool direction deviation optimization (unit: μrad)

Error item	Allowable range	Error item	Allowable range	Error item	Allowable range
ε_{XX}	[−15.6, 15.6]	ε_{XB}	[−15.4, 15.4]	S_{YZ}	[−22.5, 22.5]
ε_{YX}	[−15.9, 15.9]	ε_{YB}	[−13.3, 13.3]	S_{XZ}	[−23.1, 23.1]
ε_{XY}	[−15.6, 15.6]	ε_{ZB}	[−15.7, 15.7]	S_{BZ}	[−22.5, 22.5]
ε_{YY}	[−15.9, 15.9]	ε_{XC}	[−14.2, 14.2]	S_{CX}	[−23.1, 23.1]
ε_{XZ}	[−15.6, 15.6]	ε_{YC}	[−14.1, 14.1]	S_{CY}	[−26.6, 26.6]
ε_{YZ}	[−15.9, 15.9]	ε_{ZC}	[−15.7, 15.7]		

Total estimated cost only considering the error components above: $c_{\text{total}}=\sum_{i=1}^{18}c(T_i)=\sum_{i=1}^{18}\frac{k_i}{T_i^2}=7462941$

Thus, one can conclude that the effects of the adjusting sequence are related to the original standards of the error components that affect tool direction deviation. If the adjusting sequence of the comparative simulation is used, then when the original standard of the error components affecting tool direction deviation is lower than the directional accuracy requirement (as in the case of this study), the allocation results will be tilted towards excess precision. In contrast, when the standard is higher than the requirement, the allocation results will be tilted towards a lack of precision. Both results are not conducive to obtaining an optimal allocation scheme. However, the adjusting sequence of the formal experiment solved this exact problem. If the adjusting sequence from our proposed method is used, regardless of whether the original standard of the angular error components is higher or lower than the required accuracy, the allocation results are similar without an excess or lack of precision. Thus, the necessity of the adjusting sequence has been demonstrated.

Similarly, a total of 10000 points were randomly sampled to verify the accuracy of the allocation scheme. The results are listed in Table 12.

Table 12 Deviation statistics of the randomly sampled points within the workspace

Item	Frequency of $\lvert\Delta \boldsymbol{V}\rvert\leqslant 40$ μrad	Frequency of $\lvert\Delta \boldsymbol{P}\rvert\leqslant 20$ μm	Estimated cost
Formal experiment	95.50%	94.16%	15163102
Comparative simulation	95.59%	94.32%	16066713

These results are in line with the expectation that the positional accuracy and the estimated cost would increase, which is a situation of excess precision and waste of cost.

6 Conclusions

In this study we established a geometric error model for five-axis machine tools, comprising 41 error components, and based on the theory of muti-body systems and HTM. We also proposed a Sobol sensitivity analysis method for geometric error components in the general workspace of the machine tool.

By combining the cost and sensitivity of geometric error components, the concept of cost sensitivity

for the error components was introduced. Also, an accuracy test criterion for the tool direction and positional deviations was established, along with an algorithm to achieve the target accuracy. This approach accounts for both cost considerations and the equivalence of overall accuracy.

We suggested a two-step allocation method for the geometric error components: first, allocate those components that affect tool direction deviations, and then allocate the remaining error components. Moreover, a simulation example using a BC-type dual-rotary-table machine tool was shown to demonstrate the feasibility of the method. The simulation results showed that the accuracy allocation scheme met the target accuracy with the lowest cost. The geometric error cost was also reduced by 27.8% compared to a uniform allocation scheme, confirming the method's effectiveness. We also conducted another comparative simulation to demonstrate the necessity of the adjusting sequence derived from our method.

Acknowledgments

This work is supported by the Key R&D Program of Zhejiang Province (Nos. 2023C01166 and 2024SJCZX0046), the Zhejiang Provincial Natural Science Foundation of China (Nos. LDT23E05013E05 and LD24E050009), and the Natural Science Foundation of Ningbo (No. 2021J150), China.

Author contributions

Xiaojian LIU, Ao JIAO, Yang WANG, Guodong YI, Xiangyu GAO, Xiaochen ZHANG, Yiming ZHANG, Yangjian JI, Shuyou ZHANG, and Jianrong TAN designed the research. Ao JIAO processed the corresponding data and wrote the first draft of the manuscript. Xiaojian LIU helped to organize the manuscript. Xiaojian LIU and Ao JIAO revised and edited the final version.

Conflict of interest

Xiaojian LIU, Ao JIAO, Yang WANG, Guodong YI, Xiangyu GAO, Xiaochen ZHANG, Yiming ZHANG, Yangjian JI, Shuyou ZHANG, and Jianrong TAN declare that they have no relevant financial or non-financial interests to disclose.

References

Armillotta A, 2020. Selection of parameters in cost-tolerance functions: review and approach. *The International Journal of Advanced Manufacturing Technology*, 108(1-2): 167-182. https://doi.org/10.1007/s00170-020-05400-z

Chan K, Saltelli A, Tarantola S, 1997. Sensitivity analysis of model output: variance-based methods make the difference. Proceedings of the Winter Simulation Conference, p.261-268. https://doi.org/10.1145/268437.268489

Chen GD, Liang YC, Sun YZ, et al., 2013. Volumetric error modeling and sensitivity analysis for designing a five-axis ultra-precision machine tool. *The International Journal of Advanced Manufacturing Technology*, 68(9-12):2525-2534. https://doi.org/10.1007/s00170-013-4874-4

Chen QD, Hu XL, Lin M, et al., 2023. Research review of error compensation technology for ultra-precision machining. *China Mechanical Engineering*, 34(3):253-268 (in Chinese). https://doi.org/10.3969/j.issn.1004-132X.2023.03.001

Cheng Q, Zhao HW, Zhang GJ, et al., 2014. An analytical approach for crucial geometric errors identification of multi-axis machine tool based on global sensitivity analysis. *The International Journal of Advanced Manufacturing Technology*, 75(1-4):107-121. https://doi.org/10.1007/s00170-014-6133-8

Cheng Q, Dong LF, Liu ZF, et al., 2018. A new geometric error budget method of multi-axis machine tool based on improved value analysis. *Proceedings of the Institution of Mechanical Engineers, Part C: Journal of Mechanical Engineering Science*, 232(22):4064-4083. https://doi.org/10.1177/0954406217749269

Díaz-Saldaña G, Osornio-Ríos RA, Zamudio-Ramírez I, et al., 2023. Methodology for tool wear detection in CNC machines based on fusion flux current of motor and image workpieces. *Machines*, 11(4):480. https://doi.org/10.3390/machines11040480

Ding S, Chen ZW, Zhang H, et al., 2023. Gear evaluation deviations-based crucial geometric error identification of five-axis CNC gear form grinding process. *Journal of Manufacturing Processes*, 99:663-675. https://doi.org/10.1016/j.jmapro.2023.05.088

Fan JW, Tao HH, Pan R, et al., 2020. An approach for accuracy enhancement of five-axis machine tools based on quantitative interval sensitivity analysis. *Mechanism and Machine Theory*, 148:103806. https://doi.org/10.1016/j.mechmachtheory.2020.103806

Fan YC, Fan KC, Huang YB, 2024. Modeling and compensation of enhanced volumetric error of machine tools containing crosstalk errors. *Precision Engineering*, 86:252-264. https://doi.org/10.1016/j.precisioneng.2023.12.011

ISO (International Organization for Standardization), 2012a. Test Code for Machine Tools–Part 1: Geometric Accuracy of Machines Operating under No-Load or Quasi-Static Conditions, ISO 230-1:2012. ISO, Geneva, Switzerland.

ISO (International Organization for Standardization), 2012b. Test Code for Machine Tools–Part 7: Geometric Accuracy of Axes of Rotation, ISO 230-7:2012. ISO, Geneva, Switzerland.

Jiang XG, Cripps RJ, 2015. A method of testing position independent geometric errors in rotary axes of a five-axis machine tool using a double ball bar. *International Journal of Machine Tools and Manufacture*, 89:151-158. https://doi.org/10.1016/j.ijmachtools.2014.10.010

Li ZH, Feng WL, Yang JG, et al., 2018. An investigation on modeling and compensation of synthetic geometric errors

on large machine tools based on moving least squares method. *Proceedings of the Institution of Mechanical Engineers, Part B: Journal of Engineering Manufacture*, 232(3):412-427. https://doi.org/10.1177/0954405416645985

Lin MQ, Yuan PJ, Tan HJ, et al., 2015. Improvements of robot positioning accuracy and drilling perpendicularity for autonomous drilling robot system. IEEE International Conference on Robotics and Biomimetics, p.1483-1488. https://doi.org/10.1109/ROBIO.2015.7418980

Liu J, Tu LW, Liu GZ, et al., 2019. An analytical structural global sensitivity analysis method based on direct integral. *Inverse Problems in Science and Engineering*, 27(11): 1559-1576. https://doi.org/10.1080/17415977.2018.1531856

Niu P, Cheng Q, Liu ZF, et al., 2021. A machining accuracy improvement approach for a horizontal machining center based on analysis of geometric error characteristics. *The International Journal of Advanced Manufacturing Technology*, 112(9-10):2873-2887. https://doi.org/10.1007/s00170-020-06565-3

Niu P, Cheng Q, Liu ZF, et al., 2025. Multi-objective optimal tolerance allocation design of machine tool based on NSGA-II algorithm and thermal characteristic analysis. *Proceedings of the Institution of Mechanical Engineers, Part B: Journal of Engineering Manufacture*, 2025: 09544054241310330. https://doi.org/10.1177/09544054241310330

Saltelli A, Aleksankina K, Becker W, et al., 2019. Why so many published sensitivity analyses are false: a systematic review of sensitivity analysis practices. *Environmental Modelling & Software*, 114:29-39. https://doi.org/10.1016/j.envsoft.2019.01.012

Sobol IM, 2001. Global sensitivity indices for nonlinear mathematical models and their Monte Carlo estimates. *Mathematics and Computers in Simulation*, 55(1-3):271-280. https://doi.org/10.1016/S0378-4754(00)00270-6

Song LQ, Sun T, Jia RY, et al., 2024. An error allocation method for five-axis ultra-precision machine tools. *The International Journal of Advanced Manufacturing Technology*, 130(5-6):2601-2616. https://doi.org/10.1007/s00170-023-12756-5

Tian WJ, 2014. Investigation into Accuracy Design and Error Compensation of High-Precision Horizontal Machining Centers. PhD Thesis, Tianjin University, Tianjin, China (in Chinese).

Wang YH, Min YX, Yu GY, et al., 2023. Parameters coordinated optimization of subsynchronous oscillation of doubly fed induction generator system based on impedance sensitivity analysis with Sobol method. *High Voltage Engineering*, 49(4):1703-1713 (in Chinese). https://doi.org/10.13336/j.1003-6520.hve.20220766

Wei XY, Ye HH, Wang G, et al., 2024. Adaptive thermal error prediction for CNC machine tool spindle using online measurement and an improved recursive least square algorithm. *Case Studies in Thermal Engineering*, 56:104239. https://doi.org/10.1016/j.csite.2024.104239

Wu HR, Zheng HL, Li XX, et al., 2020a. A geometric accuracy analysis and tolerance robust design approach for a vertical machining center based on the reliability theory. *Measurement*, 161:107809. https://doi.org/10.1016/j.measurement.2020.107809

Wu HR, Zheng HL, Li XX, et al., 2020b. Robust design method for optimizing the static accuracy of a vertical machining center. *The International Journal of Advanced Manufacturing Technology*, 109(7-8):2009-2022. https://doi.org/10.1007/s00170-020-05596-0

Xia CJ, Wang SL, Sun SL, et al., 2019. An identification method for crucial geometric errors of gear form grinding machine tools based on tooth surface posture error model. *Mechanism and Machine Theory*, 138:76-94. https://doi.org/10.1016/j.mechmachtheory.2019.03.016

Xia CJ, Wang SL, Ma C, et al., 2020. Crucial geometric error compensation towards gear grinding accuracy enhancement based on simplified actual inverse kinematic model. *International Journal of Mechanical Sciences*, 169:105319. https://doi.org/10.1016/j.ijmecsci.2019.105319

Xiang ST, Wu CY, 2021. Application of sensitivity analysis in precision optimization of CNC machine tools: a state-of-the-art review. *Aeronautical Manufacturing Technology*, 64(22):40-47 (in Chinese). https://doi.org/10.16080/j.issn1671-833x.2021.22.040

Xing KL, Achiche S, Mayer JRR, 2019. Five-axis machine tools accuracy condition monitoring based on volumetric errors and vector similarity measures. *International Journal of Machine Tools and Manufacture*, 138:80-93. https://doi.org/10.1016/j.ijmachtools.2018.12.002

Xiong G, Ding Y, Zhu LM, 2019. Stiffness-based pose optimization of an industrial robot for five-axis milling. *Robotics and Computer-Integrated Manufacturing*, 55:19-28. https://doi.org/10.1016/j.rcim.2018.07.001

Yu JB, Cheng X, Lu L, et al., 2021. A machine vision method for measurement of machining tool wear. *Measurement*, 182:109683. https://doi.org/10.1016/j.measurement.2021.109683

Yuan PJ, Wang QS, Shi ZY, et al., 2014. A micro-adjusting attitude mechanism for autonomous drilling robot end-effector. *Science China Information Sciences*, 57(12):1-12. https://doi.org/10.1007/s11432-014-5190-9

Zhang HN, Xiang ST, Wu C, et al., 2024. Optimal proportion compensation method of key geometric errors for five-axis machine tools considering multiple-direction coupling effects. *Journal of Manufacturing Processes*, 110:447-461. https://doi.org/10.1016/j.jmapro.2023.12.067

Zhang K, Zhang LQ, Yan YC, 2016. Single spherical angle linear interpolation for the control of non-linearity errors in five-axis flank milling. *The International Journal of Advanced Manufacturing Technology*, 87(9-12):3289-3299. https://doi.org/10.1007/s00170-016-8720-3

Zhang Z, Jiang F, Luo M, et al., 2024. Geometric error measuring, modeling, and compensation for CNC machine tools: a review. *Chinese Journal of Aeronautics*, 37(2):163-198. https://doi.org/10.1016/j.cja.2023.02.035

Zhang ZL, Liu ZF, Cheng Q, et al., 2017. An approach of comprehensive error modeling and accuracy allocation for the improvement of reliability and optimization of cost

of a multi-axis NC machine tool. *The International Journal of Advanced Manufacturing Technology*, 89(1-4):561-579. https://doi.org/10.1007/s00170-016-8981-x

Zhong XM, Liu HQ, Mao XY, et al., 2019. Influence and error transfer in assembly process of geometric errors of a translational axis on volumetric error in machine tools. *Measurement*, 140:450-461. https://doi.org/10.1016/j.measurement.2019.04.032

Zhu MR, Yang Y, Feng XB, et al., 2023. Robust modeling method for thermal error of CNC machine tools based on random forest algorithm. *Journal of Intelligent Manufacturing*, 34(4):2013-2026. https://doi.org/10.1007/s10845-021-01894-w

Electronic supplementary materials

Section S1, Fig. S1